Projections of future floods and hydrological droughts in Europe under a +2°C global warming

Philippe Roudier, Jafet C. M. Andersson, Chantal Donnelly, Luc Feyen, Wouter Greuell, Fulco Ludwig

Projections of future floods and hydrological droughts in Europe under a +2°C global warming

Philippe Roudier[1,*], Jafet C.M. Andersson[2], Chantal Donnelly[2], Luc Feyen[3], Wouter Greuell[4], Fulco Ludwig[4]

1. Sorbonne Universités (UPMC, Univ Paris 06)-CNRS-IRD-MNHN, LOCEAN/IPSL, 4 place Jussieu, F-75005 Paris, France

2. Swedish Meteorological and Hydrological Institute (SMHI), Norrköping, Sweden.

3. Climate and Risk Management Unit, Institute for Environment and Sustainability (IES), Joint Research Centre (JRC), European Commission (EC), Ispra, Italy.

4. Earth System Sciences group, Wageningen University and Research centre (WUR), Wageningen, The Netherlands

*Corresponding author: philippe.roudier@locean.upmc.fr, tel: +33 144272711

Abstract

We present an assessment of the impacts of a +2°C global warming on extreme floods and hydrological droughts (1 in 10 and 1 in 100 year events) in Europe using eleven bias-corrected climate model simulations from CORDEX Europe and three hydrological models. The results show quite contrasted results between northern and southern Europe. Flood magnitudes are expected to increase significantly south of 60°N, except for some regions (Bulgaria, Poland, south of Spain) where the results are not significant. The sign of these changes are particularly robust in large parts of Romania, Ukraine,

Germany, France and North of Spain. North of this line, floods are projected to decrease in most of Finland, NW Russia and North of Sweden, with the exception of southern Sweden and some coastal areas in Norway where floods may increase. The results concerning extreme droughts are less robust, especially for drought duration where the spread of the results among the members is quite high in some areas. Anyway, drought magnitude and duration may increase in Spain, France, Italy, Greece, the Balkans, south of the UK and Ireland. Despite some remarkable differences among the hydrological models' structure and calibration, the results are quite similar from one hydrological model to another. Finally, an analysis of floods and droughts together shows that the impact of a +2°C global warming will be most extreme for France, Spain, Portugal, Ireland, Greece and Albania. These results are particularly robust in southern France and northern Spain.

1. Introduction

In Europe, freshwater resources are of crucial importance for many sectors including agriculture, hydropower generation, cooling water for power plants and domestic and industrial water supply. At the same time, water can have a direct impact on safety and livelihoods through floods that can lead to disastrous human and economic losses (e.g. the 2013 floods in Central Europa resulted in a loss of more than €12bn[1]). During the last decades, several studies have underlined that water resources and especially river flows have had strong variations across Europe (Kovats et al., 2014) due to climate, water extractions and land use change (Sterling et al., 2013). Even if the relative share of these three driving factors is difficult to assess over the past, it is clear that the strong climate changes expected in Europe for the 21st century will have a significant impact on river flows (Jiménez Cisneros et al., 2014).

[1] http://www.munichre.com/en/media-relations/publications/press-releases/2013/2013-07-09-press-release/index.html

43 Thus, a first step in order to make relevant mitigation and adaptation policies is to develop a clear
44 picture of the potential future stream flows extremes.

45 Changes in river flow extremes at a +2°C global warming are currently of central interest as this is
46 the global target defined by policymakers to lower international greenhouse gases emissions (European
47 Commission, 2007). Therefore, in this study, we do not select a specific time period; rather we focus on
48 defining the hydrological impacts in a world with a +2°C global warming relative to pre-industrial levels
49 (Vautard et al., 2014). Describing the impacts of a +2°C global warming on topics such as water
50 resources, agriculture or infrastructures is the main aim of the FP7 project IMPACT2C under which this
51 study was conducted.

52 Future changes in hydrological extremes are still highly uncertain. There is a general consensus that
53 in most part of the world climate change will result in more rainfall extremes (IPCC, 2012). However, to
54 what extent this will affect hydrological extremes is still highly uncertain and differs from region to
55 region. To address this uncertainty many previous studies have used multiple climate models to force a
56 single hydrological model (e.g. Dankers and Feyen (2009); Feyen et al. (2009)). However recent work,
57 mainly at global scale, has shown that not only the choice of the climate models affect future change in
58 hydrological extremes: different hydrological models give sometimes very different results too
59 (Haddeland et al. (2011); Schewe et al. (2014); Prudhomme et al. (2014); Dankers et al. (2014)). Many
60 multiple climate and hydrological models impact assessments have used global climate models. These
61 global climate models tend to have significant biases in the representation of precipitation extremes.
62 The aim of this study is to improve the assessment of hydrological extreme impacts at the European
63 continent scale including a better description of uncertainties through the use of multiple hydrological
64 models and state-of-the art climate projections from the high-resolution CORDEX project. We first focus
65 on the skill of each hydrological model to simulate extreme floods and hydrological drought (section 3.1)

and we next assess the impact that a +2°C warming would have on meteorological variables which are relevant for flood and drought generation (section 3.2) and on extreme flows (return periods are 10 and 100 years, section 3.3 and 3.4). We finally summarize the results about flood magnitude, droughts magnitude and drought duration for twelve European cities and with a final assessment on which European region will be the most affected by extreme flows at +2°C warming.

2. Material and data

2.1 Data

2.1.1 Forcing data

This study uses a sub-ensemble from the latest (as of 2014) ensemble of high-resolution, dynamically downscaled daily climate simulations from CMIP5, 5th Coupled Model Intercomparison Project and CORDEX, A Coordinated Regional Downscaling Experiment (Jacob et al., 2014). The 11 ensemble members were chosen to be representative of the larger ensemble and consist of 5 GCM/RCM combinations and 3 Representative Concentration Pathways (RCPs) (Moss et al. (2010)) (Table 1). One of the main differences with previous impact studies is that rather than focusing on a future time slice, change is quantified at the 30-year period when each driving GCM reaches +2°C in global mean temperature relative to pre-industrial levels (1881-1910, Vautard et al. (2014)). Thus, the ensemble is a representation of a world where greenhouse gas emissions have caused a +2°C global warming. The climate variables were regridded to a 0.25° resolution grid. As climate models are known to be affected by some biases that can clearly affect the results (Chen et al., 2013), daily climate

89 variables (precipitation, maximum, minimum and average temperature, dew point temperature,
90 shortwave and longwave downward radiations) were bias-corrected using quantile mapping (Themeßl
91 et al. (2011), Themeßl et al. (2012) and Wilcke et al. (2013)). Bias-correction was made using the E-OBS
92 gridded observational dataset (Haylock et al., 2008) as a reference. These bias corrected data were then
93 used to run the three hydrological models (1971-2100). Climatic changes were subsequently assessed by
94 comparing the +2°C period with the baseline period 1971-2000 (Table 1).

95 #### 2.1.2 Observed discharge data

96 In order to assess the skills of the hydrological models in representing specific floods and
97 droughts, we used 428 discharge stations over Europe selected from the Joint Research Center database
98 which gathers several sources like the Global Runoff Data Centre (2013) data or other publicly available
99 datasets *(*e.g., HYDROBanque, CEDEX, Norwegian Water Resources and Energy Directorate, National
100 river flow archive, Waterinfo.be , eHyd*)*. The original database was filtered to include only stations with
101 data for the time period 1971-2000 and with no day with missing data in order to not to miss any
102 extreme discharges. Model performance was validated using the median of the values from each
103 hydrological model forced by the ensemble of climate models over the 30 years control period.

104

105 ### 2.2 Summary of models

106 Three pan-European hydrological models were used to simulate daily discharge: Lisflood (Burek
107 et al., 2013), E-Hype (Donnelly et al., 2015) and VIC (Liang et al., 1994). The models differ in both
108 complexity of process description, input data and setup. For example, differences include spatial
109 resolution (one model is subbasin rather than grid based), description of evapotranspiration and snow
110 processes, the number of soil layers and depth assumptions and the calibration procedure. A summary
111 of these models can be found in the Appendix and more details are available in Greuell et al. (2015).

Because each of these models has a different output resolution (and in the case of E-HYPE, a high-resolution subbasin rather than grid output), the output from each model was regridded to a comparable 0.5°*0.5° grid.

2.3 Methodology for extreme value analysis

2.3.1 High flows

We focus here on the discharge magnitude of the 1 in 10 and 1 in 100 year floods (QRP10 and QRP100). These two return periods were chosen as the first one represents an extreme event occurring often enough that it is remembered by individuals and communities and the other one is a standard value used in some countries to design flood protection. In order to compute QRP10 and QRP100 for each pixel of the grid, we followed a typical extreme value analysis fitting methodology (see e.g. Roudier and Mahé (2010)). First, the daily maximum discharge was selected for each year of the 30 years long period, then fitted a Generalized Extreme Value (GEV) distribution using the L-moments and finally, we calculated QRP10 and QRP100 using the fitted function. The goodness-of-fit was also checked using the Anderson-Darling test (at 5%), as recommended by Meylan et al. (2008). For each of the 3 hydrological models, and each of the 11 climate runs, the relative QRP10 and QRP100 change between the +2°C period and the baseline was computed, resulting in a set of 33 relative changes. To describe this set, in this paper the median of all the ensemble members is used (the combined climatological and hydrological model ensemble) rather than the mean, in order to avoid giving excessive weight to potential outliers. The significance of changes is also assessed using a Wilcox test (5% threshold) between future period and baseline. Therefore, in all relative change plots, we set as missing values

pixel that do not pass the test. Moreover, those that do not pass the goodness-of-fit test were also set as missing value.

2.3.2 Low flows

We focus for low flows on the same return periods as for the high flow analysis, following the methodology used by Feyen and Dankers (2009). First the daily discharge time-series is smoothed applying a seven day moving average in order to remove the day-to-day variations and then for the magnitudes of low flows (QlowRP10 and QlowRP100), the lowest smoothed discharge event is selected, every year. For the duration of low flows a threshold approach is used with the 20^{th} flow percentile of the smoothed flow duration curve as threshold. After computing the 20^{th} percentile (for each pixel, projection and hydrological model) we select all the days that have a smoothed discharge value below this 20^{th} percentile and then we compute the duration of each event below that threshold and select the maximum drought duration for each year. Finally, for both drought magnitude and duration, the rest of the methodology is equal to section 2.3.1 (fitting a GEV distribution on each set of 30 values in order to compute QlowRP10 and QlowRP100 magnitude and duration; we also set as missing values pixel that do not pass the Wilcox or Anderson-Darling test)

3. Results and discussion

3.1 Hydrological model validation and selection for ensemble projections

A broad and detailed validation of the hydrological models focusing on average conditions is presented in Greuell et al. (2015). The aim of the validation presented here is to assess the models' skill to simulate specific indicators used in this study. For each hydrological model we therefore assess if the median QRP100 (QlowRP100) computed based on the 11 bias corrected climate runs is close to the QRP100 (QlowRP100) computed with observed discharge data. Results are shown in Figure S1 (see supplementary material) for floods and Figure S2 for low flows. The skills of the three hydrological models are generally better for high than low flows. Lisflood performs slightly better than the other models, according to the Nash-Sutcliffe Efficiency coefficient (NSE = 0.82) and the Root Mean Squared Error (RMSE = 961 m3/s). However, when focusing on the NSE of the logarithmic modeled and observed values (NSE(log), used for extreme values, see Krause et al., (2005)), E-Hype is slightly better than Lisflood. For low flows, Lisflood somewhat overestimates QlowRP100 while the other two models underestimate it. E-Hype has the best performance for low flows (NSE = 0.72, NSE(log)=0.68, RMSE = 75 m3/s) compared to Lisflood (NSE=0.54, NSE(log)=0.51, RMSE=95 m3/s) and VIC (NSE=0.38, NSE(log)=0.38, RMSE=112 m3/s).

A likely explanation for these differences in performance could be the way these models are tuned to observation data. The Lisflood model is calibrated in individual catchments using a high-resolution (5 km) interpolated observation data set (EFAS-meteo, see Ntegeka et al. (2013)) and default parameters in ungauged catchments. The VIC model uses a general set of parameters applicable anywhere in the model domain, but linked to soil-type and landuse. This parameter tuning was done using a specific forcing dataset described in Nijssen et al. (2001) .The E-HYPE model also uses a general set of parameters, linked to soil-type and landuse. For E-HYPE, these parameters were originally calibrated to a small set of representative gauged basins for each soil and land use using a corrected ERA-INTERIM forcing data set (see Donnelly et al. (2015)), but for this study an evapotranspiration parameter was slightly adjusted to better balance the model performance with the E-OBS data set. This

was deemed important by the E-HYPE modeling team as the climate scenarios were bias-corrected to the E- OBS data set and recent studies have shown that bias-correction and climate impact results can vary between reference observation data sets (e.g. Gutmann et al. (2014)). It is therefore not surprising that overall E-HYPE performs well when forced with data bias-corrected to E-OBS, at least regarding mean discharge. Lisflood is likely to perform better in regions where the E-OBS forcing is not significantly different to the EFAS-meteo data as the other models compromise performance in individual catchments for relatively good performance in multiple catchments using the same parameters. For hydrological extremes, again Lisflood can be expected to perform well in calibration catchments. E-HYPE may outperform VIC for extremes because the representative gauged basins used to calibrate E-HYPE are generally smaller catchments (1000 to 5000 km^2) where runoff generating processes dominate over routing and lake processes.

Given the variability in model performance for extremes, and perhaps inability of some models to successfully represent these extremes, we suggest to remove for the initial selection the hydrological models that have a NSE and a NSE(log) below 0.5 for the index studied, i.e. QRP100 and QlowRP100. Based on the NSE threshold, an ensemble consisting of results from E-HYPE, Lisflood, and VIC will be used for floods, and Lisflood and E-HYPE for low flows.

3.2 Summary of projected changes in meteorological variables pertaining to floods and droughts

We first aim at studying here the future evolution of some of the drivers of low and high flow changes. We therefore plot in Figure 1 the projected change in maximum annual snowpack (outputs from the 3 hydrological models) and intense daily rainfall (return period is 10 years, computed using a GEV distribution using the aforementioned methodology for discharge) at +2°C warming. Results show that there is generally a clear decrease in maximum snowpack, reflecting the future warming over Europe. The regions that are less affected like southern Spain or southern Italy are those with currently

204 marginal snowfall. The snowpack decrease is particularly important in Fenno-Scandinavia and the Alps.
205 Intense rainfall events are projected to increase significantly over the whole continent, with no
206 particular spatial pattern, which is consistent with previous studies (Madsen et al. (2014); Rajczak et al.
207 (2013)).

208

209 3.3 Floods (QRP10 and QRP100)

210 For changes in flood magnitude there is a clear North to South gradient, with a strong increase
211 with a strong increase in flood magnitudes south the 60°N line, except for some regions in Bulgaria,
212 Czech Republic, Poland, the western Balkans, the Baltic countries, and southern Spain where no
213 significant changes can be detected (Figure 2). Almost everywhere the increase in 100 year floods
214 (QRP100) is stronger than the 10 year floods (QPR10). Floods are even increasing in areas such as
215 southern Mediterranean where the average discharge is projected to decrease (Greuell et al., 2015).
216 However flood changes are consistent with the extreme rainfall changes south of 60°N (Figure 1). Above
217 the 60^{o}N line, the situation is more heterogeneous with a relatively strong decrease in flood magnitude
218 in parts of Finland, NW Russia and North of Sweden with the exception of southern Sweden and some
219 coastal areas in Norway where increases in floods are projected. Projections of decreasing flood
220 magnitudes are mainly due to the decreases in snowpack in areas where most of the floods are caused
221 by spring snowmelt in combination with rainfall. Increases in flood magnitude in Scandinavia are mainly
222 seen in coastal areas where the rain-fed floods will increase (similar results were found by Vormoor et
223 al. (2015)). Note also that the date of occurrence of annual maximum discharge is expected to be earlier
224 in spring for these areas (Figure S8) while for the rest of Europe, changes are quite limited.

225 Following this reduction in snow-melt floods in Fenno-Scandinavia and according to the
226 decreasing snow pattern shown in Figure 1, it is expected a similar decrease in floods would be expected

for the Alps. However, our results shown an increase in floods which is also reported in several other studies (Rojas et al. (2012), Gobiet et al. (2014) or Köplin et al. (2014)). For Switzerland, Köplin et al. (2014) showed that there are large contrasts in the flood regime in the Alps, and snowmelt-floods only occur in a limited part of country. Thus, at a 0.5°*0.5° resolution, we are not able to capture some local decreases of QRP10 and QRP100 due to earlier snowmelt. This hypothesis is confirmed by the same analysis performed only for Lisflood at 5*5 km grid that shows for some areas a decrease of QRP100. Secondly, we think that at the 0.5°*0.5° resolution over the Alps, there is for most of the pixels a change of flood regime (from snowmelt to rain-fed or mixed snowmelt-rain-fed) rather than only an earlier occurrence of snowmelt floods, leading to a different situation compared to Fenno-Scandinavia. This hypothesis, is supported by Figure S8 which shows (i) a clear reduced number of high flows in June (southern Alps) and July (rest of the Alps) but (ii) no strong increase in earlier spring. A deeper analysis, at a finer scale, is needed to fully understand all the changes in the Alps but beyond the scope of the present paper.

Finally, we also provide model-by-model details of these results in the Appendix. Generally, all three hydrological models show the same pattern. However, in Western Europe and the Mediterranean area, Lisflood projects a stronger flood increase than the other models.

Even if it is difficult to compare with studies that do not focus on exactly the same set of parameters (climate models, resolution, time period), these results are mainly in line with the recent literature as reviewed by Madsen et al. (2014) (table 3 in their paper). Out of 22 studies dealing with future flood projections in Europe, 4 of them are not directly comparable (they differentiate winter and spring floods), 14 have a global agreement with our findings and 4 give different results. Those four studies include (i) the UK, where Reynard et al. (2010) find few catchments with changes in flood frequency above +20% and Kay et al. (2006), with a limited ensemble of driving climate runs, depict a

250 decrease in flood magnitude in south and east England; (ii) France (Seine and Somme rivers) where
251 Ducharne et al. (2010) cannot conclude on any robust change while we find a significant increase of
252 flood events and (iii) eastern Germany, Poland and southern Sweden where Rojas et al. (2012) find
253 decreases in flood magnitude (this latter study which covers the whole continent agrees however with
254 our results for the rest of Europe). Finally, Dankers et al. (2014) find more contrasted changes for 1 in 30
255 year flood change in Europe using several GCMs and hydrological models: according to these results,
256 floods would decrease in large parts of Europe including Greece, Italy and eastern Europe.

257

258 3.4 Low flows: magnitude and duration

259 Low floods (QlowRP10) are expected to decrease for many countries mainly located in the
260 southern part of Europe: Spain, France, Italy, Greece, the Balkans and also south of the UK and Ireland.
261 This is mainly due to less rainfall (Rajczak et al., 2013) and also higher potential evapotranspiration in
262 some regions like Italy (see Figure S4 and Van Vliet et al.,2015). The duration of these droughts is also
263 increasing (Figure 3, top), especially in Spain. For the rest of Europe, the projections show generally a
264 decrease of drought magnitude and duration. Moreover, changes are not significant in some areas like
265 western Germany or southern Sweden: areas with in-significant changes are larger for low flows than
266 for floods. This reduction of low flow duration and magnitude is mainly caused (i) by less snowfall and
267 more precipitation for areas with low flows in winter and (ii) by a general increase of rainfall for areas
268 with low flows in summer (Vautard et al., 2014). Both hydrological models depict generally the same
269 pattern (see Figure S5 for magnitude). However, for southern Sweden, E-HYPE predicts a small decrease
270 in low-flow magnitudes and Lisflood an increase. Lisflood also tends to predict a significant increase of
271 QlowRP10 across Eastern Europe while for E-HYPE this change is also positive, but not significant (white

pixels). The same spatial pattern is found for the 100 year return period (see Figure S6) but the results are generally less significant, see for example southern France.

Our results on drought magnitude change are similar to those presented by Forzieri et al. (2014). Focusing on the QlowRP20 they also find for the 2080s a decrease for the Mediterranean and the UK but their findings for Sweden and Norway show an almost uniform increase of low flows although we observed a North/South difference that may reflect the different set of climate models used. Prudhomme et al. (2014), using several climate and hydrological models find a general increase of hydrological droughts over Europe, but they focus on less extreme droughts, and they use RCP 8.5, at the end of the century. At a more local scale, other studies agree with our results. For example, in France, Chauveau et al. (2013) also predict a decrease in low flow magnitude; in Germany Huang et al. (2014) find a decrease of QlowRP50 in 2080 for some areas like the Rhine basin and uncertainty elsewhere.

3.5 Uncertainties and summary of the results

We analyzed the spread in future change of hydrological extremes using three different parameters (QRP10, QlowRP10 and QlowRP10 duration) and focusing on the 1st and 3rd quartiles of relative changes distribution (Figure 4 and Figure S7). The spread among results is the largest for QlowRP10 duration, depicted in Figure 4 by the inter-quartile range. Despite this spread, the sign of QlowRP10 duration change (positive or negative) is the same for the first and third quartiles for areas with a very large spread (e.g. eastern Europe), i.e. the ensemble of projections somewhat agree on the direction of change, but uncertainty is high. Second, for QlowRP10 magnitude the spread between both quartiles is generally smaller especially in areas like France, the UK, Italy, Portugal and Greece where it is generally below 20%. However, both quartiles do not have the same sign in all these areas (e.g. the UK and Italy) thus depicting projections less robust than for Portugal, south of France or south of Spain.

Third, for floods (QRP10) the quartiles agreement is slightly better than for QlowRP10 magnitude except in southern Fenno-scandinavia This general larger uncertainty for low flows is mainly due to (i) differences between the two models in soil moisture and evapotranspiration calculation which are directly related to low flows (Greuell et al., 2015) and (ii) the number of selected models is different for floods (VIC, E-HYPE, Lisflood) and droughts (E-HYPE, Lisflood). Figure S1 and Figure S2 show clearly that the three hydrological models perform similar for floods while for droughts, Lisflood tends to overestimate QlowRP10 and E-HYPE to underestimate it, thus resulting in a larger spread. Moreover, with this kind of assessment using quartiles, the areas with robust results are generally the same than the ones using the Wilcox test, except for some areas like southern Spain where this latter test gives significant changes.

In order to detect hotspot regions that will be subject to negative changes in several extreme flow indicators, we combined the floods, drought magnitude and drought duration changes in a single analysis (Figure 5). In most parts of France, Spain, Portugal, Ireland, Greece and Albania, the projected changes under +2°C are generally more extreme. We mean by "more extreme" regions where there is a consistent worsening (of at least 5%) in all the extreme indicators considered for a 10-years return period: more intense floods (QRP10 >+5%), more intense hydrological droughts (QlowRP10<-5%) and longer droughts (QlowRP10 duration > +5%). In parts of Norway, Sweden, Finland and western Russia future warming will see a reduction in both streamflow floods and droughts.

4. Conclusion

Our aim is to make a robust assessment of the impact that a +2°C global warming would have on hydrological extremes (floods, droughts magnitude and duration) in Europe by using an ensemble of eleven high-resolution RCM outputs and three pan-European hydrological models. Results show that

318 such a warming could increase flood magnitudes (10 years and 100 years return period) significantly in
319 most parts of Europe (e.g. about +20% close to London; and Warsaw for QRP10), even for areas where
320 the annual rainfall is expected to decrease in the future, e.g. Spain (about +10% QRP10 close to Sevilla).
321 However, in Fenno-Scandinavia the situation is more contrasted with (i) a large area that is expected to
322 have less intense snowmelt floods, occurring earlier in spring except and (ii) the southern and coastal
323 areas of Fenno-Scandinavia where we predict an increase of rain-fed flood magnitude. In the Alps, even
324 though snowpack is also projected to reduce, floods are expected to increase generally due to a change
325 of flood regime from snowmelt to rain-fed and possibly because the spatial resolution of this study
326 (0.5°*0.5°) potentially hides local decreases of intense snowmelt floods. Moreover, despite some
327 significant differences among the hydrological models' structure and calibration, the results are quite
328 similar from one model to another and consistent with other studies.

329 Future changes in hydrological drought magnitude and duration show contrasting patterns across
330 Europe. Our projections show that for large areas of Italy, France, Spain, Greece, the Balkans, Ireland
331 and the UK, droughts will become more intense and longer mainly due to less rainfall and higher
332 evapotranspiration, in some areas. The sign of these changes is particularly robust in southern France,
333 parts of Spain, Portugal and Greece. For the rest of Europe changes in droughts are not significant or
334 there is a reduction of droughts length and magnitude, especially in northern Fenno-Scandinavia and
335 Western Russia where the sign of the changes is also very robust.

336 Our results show that for a significant part of Europe there will be a clear intensification of the
337 hydrological cycle resulting in both increases in droughts and floods. Extreme flows will be particularly
338 harmful in Spain, Greece, France, Ireland and Albania: it is thus urgent to integrate these future changes
339 for policy making in water resources management and flood protection design.

340

Acknowledgments

The authors would like to thank the FP7 project IMPACT2C and all the contributing members for funding this study and providing climate data. Moreover, we thank Goncalo Gomes from JRC for his help with observed discharges and Alessandra Bianchi for GIS support. We finally think three anonymous reviewers for their helpful comments.

References

Burek P, van der Knijff J, de Roo A (2013) LISFLOOD Distributed Water Balance and Flood Simulation Model. Revised user manual. JRC technical reports EUR 22166 EN/3 EN

Chauveau M, Chazot S, Perrin C, Bourgin PY, Sauquet E (2013) Quels impacts des changements climatiques sur les eaux de surface en France a l'horizon 2070 ? La Houille Blanche - Revue internationale de l'eau:5-15

Chen J, Brissette FP, Chaumont D, Braun M (2013) Finding appropriate bias correction methods in downscaling precipitation for hydrologic impact studies over North America. Water Resources Research 49:4187-4205 doi:10.1002/wrcr.20331

Dankers R, Feyen L (2009) Flood hazard in Europe in an ensemble of regional climate scenarios. Journal of Geophysical Research: Atmospheres, 114, 10.1029/2008jd011523

Dankers R et al. (2014) First look at changes in flood hazard in the Inter-Sectoral Impact Model Intercomparison Project ensemble. Proceedings of the National Academy of Sciences 111:3257-3261 doi:10.1073/pnas.1302078110

Donnelly C, Andersson JCM, Arheimer B (2015) Using flow signatures and catchment similarities to evaluate the E-HYPE multi-basin model across Europe. Hydrological Sciences Journal doi:10.1080/02626667.2015.1027710

363 Ducharne A et al. Climate change impacts on water resources and hydrological extremes in northern
364 France. In: Carrera J (ed) Proceedings of the XVIII International Conference on Computation
365 Methods in Water Resources, Barcelona, Spain, 21–24 June 2010.
366 European Commission (2007) Limiting global climate change to 2 degrees Celsius: the way ahead for
367 2020 and beyond. Commission of the European Communities, Brussels, Belgium
368 Feyen L, Barredo JI, Dankers R (2009) Implications of global warming and urban land use change on
369 flooding in Europe, Water and Urban Development Paradigms, edited by: Feyen, J., Shannon, K.,
370 and Neville, M., 217-225 pp.
371 Feyen L, Dankers R (2009) Impact of global warming on streamflow drought in Europe. Journal of
372 Geophysical Research: Atmospheres 114:D17116 doi:10.1029/2008jd011438
373 Forzieri G, Feyen L, Rojas R, Flörke M, Wimmer F, Bianchi A (2014) Ensemble projections of future
374 streamflow droughts in Europe. Hydrology and Earth System Sciences 18:85-108
375 doi:10.5194/hess-18-85-2014
376 Global Runoff Data Centre (2013) Long-Term Mean Monthly Discharges and Annual Characteristics of
377 GRDC Station. Global Runoff Data Centre, Federal Institute of Hydrology (BfG), Koblenz,
378 Germany
379 Gobiet A, Kotlarski S, Beniston M, Heinrich G, Rajczak J, Stoffel M (2014) 21st century climate change in
380 the European Alps—A review. Science of The Total Environment 493:1138-1151
381 doi:http://dx.doi.org/10.1016/j.scitotenv.2013.07.050
382 Greuell W et al. (2015) Evaluation of five hydrological models across Europe and their suitability for
383 making projections underof climate change. Hydrology and Earth System Sciences Discussion 12,
384 10289-10330, doi:10.5194/hessd-12-10289-2015

385 Gutmann E, Pruitt T, Clark MP, Brekke L, Arnold JR, Raff DA, Rasmussen RM (2014) An intercomparison
386 of statistical downscaling methods used for water resource assessments in the United States.
387 Water Resources Research 50:7167-7186 doi:10.1002/2014wr015559
388 Haddeland I et al. (2011) Multimodel Estimate of the Global Terrestrial Water Balance: Setup and First
389 Results. Journal of Hydrometeorology 12:869-884 doi:10.1175/2011jhm1324.1
390 Haylock MR, Hofstra N, Klein Tank AMG, Klok EJ, Jones PD, New M (2008) A European daily high-
391 resolution gridded data set of surface temperature and precipitation for 1950–2006. Journal of
392 Geophysical Research: Atmospheres 113 doi:10.1029/2008jd010201
393 Huang S, Krysanova V, Hattermann F (2014) Projections of climate change impacts on floods and
394 droughts in Germany using an ensemble of climate change scenarios. Regional Environmental
395 Change doi:10.1007/s10113-014-0606-z
396 IPCC (2012) Managing the Risks of Extreme Events and Disasters to Advance Climate Change Adaptation.
397 A Special Report of Working Groups I and II of the Intergovernmental Panel on Climate Change
398 Cambridge, UK and New York, NY, USA
399 Jacob D et al. (2014) EURO-CORDEX: new high-resolution climate change projections for European
400 impact research. Regional Environmental Change 14:563-578 doi:10.1007/s10113-013-0499-2
401 Jiménez Cisneros BE et al. (2014) Freshwater resources. In: Field CB et al. (eds) Climate Change 2014:
402 Impacts, Adaptation, and Vulnerability. Part A: Global and Sectoral Aspects. Contribution of
403 Working Group II to the Fifth Assessment Report of the Intergovernmental Panel on Climate
404 Change. Cambridge University Press, Cambridge, United Kingdom and New York, NY, USA, pp
405 229-269
406 Kay AL, Reynard NS, Jones RG (2006) RCM rainfall for UK flood frequency estimation. I. Method and
407 validation. Journal of Hydrology 318:151-162
408 doi:http://dx.doi.org/10.1016/j.jhydrol.2005.06.012

409 Krause P, Boyle DP, Bäse F (2005) Comparison of different efficiency criteria for hydrological model
410 assessment. Advances in Geosciences, 5, 89-97, doi:10.5194/adgeo-5-89-2005
411 Köplin N, Schädler B, Viviroli D, Weingartner R (2014) Seasonality and magnitude of floods in Switzerland
412 under future climate change. Hydrological Processes 28:2567-2578 doi:10.1002/hyp.9757
413 Kovats RS et al. (2014) Europe. In: Barros VR et al. (eds) Climate Change 2014: Impacts, Adaptation, and
414 Vulnerability. Part B: Regional Aspects. Contribution of Working Group II to the Fifth Assessment
415 Report of the Intergovernmental Panel on Climate Change. Cambridge University Press,
416 Cambridge, United Kingdom and New York, NY, USA, pp 1267-1326
417 Liang X, Lettenmaier DP, Wood EF, Burges SJ (1994) A simple hydrologically based model of land surface
418 water and energy fluxes for general circulation models. Journal of Geophysical Research:
419 Atmospheres (1984–2012) 99:14415-14428
420 Madsen H, Lawrence D, Lang M, Martinkova M, Kjeldsen TR (2014) Review of trend analysis and climate
421 change projections of extreme precipitation and floods in Europe. Journal of Hydrology 519, Part
422 D:3634-3650 doi:http://dx.doi.org/10.1016/j.jhydrol.2014.11.003
423 Meylan P, Favre A-C, Musy A (2008) Hydrologie Frequentielle. Science et ingénierie de l'environnement.
424 PPUR
425 Moss RH et al. (2010) The next generation of scenarios for climate change research and assessment.
426 Nature 463:747-756
427 Nijssen B, Schnur R, Lettenmaier DP (2001) Global Retrospective Estimation of Soil Moisture Using the
428 Variable Infiltration Capacity Land Surface Model, 1980–93. Journal of Climate 14:1790-1808
429 Ntegeka V, Salamon P, Gomes G, Sint H, Lorini V, Zambrano-Bigiarini M, Thielen J (2013) EFAS-Meteo: A
430 European daily high-resolution gridded meteorological data set for 1990 – 2011. Report EUR
431 26408 EN

Prudhomme C et al. (2014) Hydrological droughts in the 21st century, hotspots and uncertainties from a global multimodel ensemble experiment. Proceedings of the National Academy of Sciences 111:3262-3267 doi:10.1073/pnas.1222473110

Rajczak J, Pall P, Schär C (2013) Projections of extreme precipitation events in regional climate simulations for Europe and the Alpine Region. Journal of Geophysical Research: Atmospheres 118:3610-3626 doi:10.1002/jgrd.50297

Reynard NS, Crooks SM, Kay AL, Prudhomme C (2010) Regionalised Impacts of Climate Change on Flood Flows. Department for Environment, Food and Rural Affairs

Rojas R, Feyen L, Bianchi A, Dosio A (2012) Assessment of future flood hazard in Europe using a large ensemble of bias-corrected regional climate simulations. Journal of Geophysical Research: Atmospheres 117:D17109 doi:10.1029/2012jd017461

Roudier P, Mahé G (2010) Calculation of design rainfall and runoff on the Bani basin (Mali) : a study of the vulnerability of hydraulic structures and of the population since the drought. Hydrological Sciences Journal 55:351–363

Schewe J et al. (2014) Multimodel assessment of water scarcity under climate change. Proceedings of the National Academy of Sciences 111:3245-3250 doi:10.1073/pnas.1222460110

Sterling S, Ducharne A, Polcher J (2013) The impact of global land-cover change on the terrestrial water cycle. Nature Climate Change 3:385-390

Themeßl M, Gobiet A, Heinrich G (2012) Empirical-statistical downscaling and error correction of regional climate models and its impact on the climate change signal. Climatic Change 112:449-468 doi:10.1007/s10584-011-0224-4

Themeßl M, Gobiet A, Leuprecht A (2011) Empirical-statistical downscaling and error correction of daily precipitation from regional climate models. International Journal of Climatology 31:1530-1544 doi:10.1002/joc.2168

Van Vliet M, Donnelly C, Stromback L, Capell R (submitted) European scale climate information services for water use sectors. Journal of Hydrology

Vautard R et al. (2014) The European climate under a 2 °C global warming. Environmental Research Letters 9:034006

Vormoor K, Lawrence D, Heistermann M, Bronstert A (2015) Climate change impacts on the seasonality and generation processes of floods - projections and uncertainties for catchments with mixed snowmelt/rainfall regimes. Hydrology and Earth System Sciences 19:913-931 doi:10.5194/hess-19-913-2015

Wilcke R, Mendlik T, Gobiet A (2013) Multi-variable error correction of regional climate models. Climatic Change 120:871-887 doi:10.1007/s10584-013-0845-x

483

484

485

486 **Tables**

487

RCM	Driving GCM	RCP	+2°C period
CSC-REMO2009	MPI-ESM-LR	8.5	2030-2059
		4.5	2050-2079
		2.6	2071-2100
SMHI-RCA4	HadGEM2-ES	8.5	2016-2045
		4.5	2023-2053
SMHI-RCA4	EC-EARTH	8.5	2027-2056
		4.5	2042-2071
		2.6	2071-2100
KNMI-RACMO22E	EC-EARTH	8.5	2028-2057
		4.5	2042-2071
IPSL-WRF331F	IPSL-CM5A-MR	4.5	2028-2057

488 **Table 1: Summary of the 11 climate projections used in this study (RCP, GCM, RCM and +2°C period)**

489

490

491

492

493 **Figures**

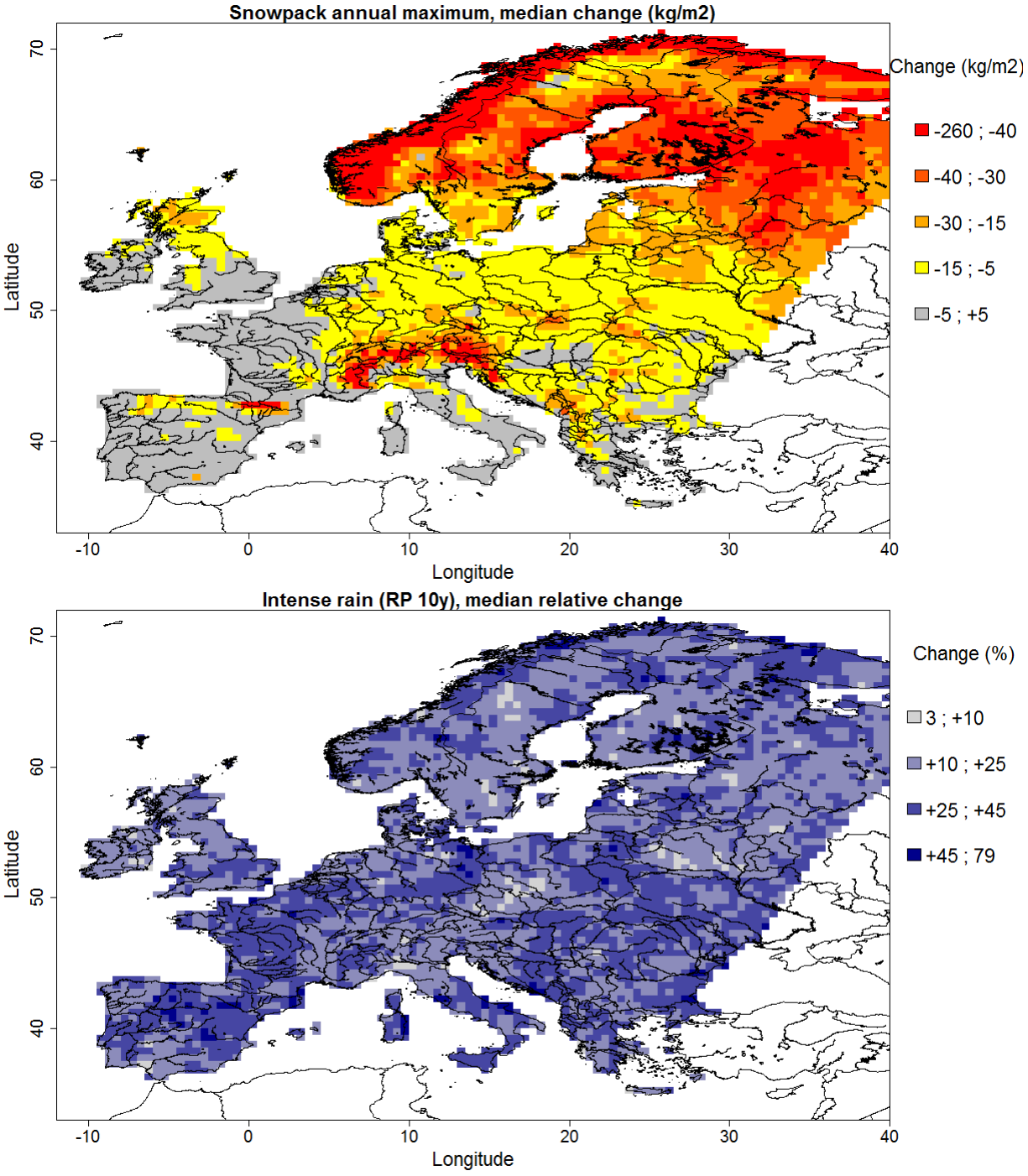

494

495 **Figure 1: Change in maximum annual snowpack (all three hydrological models, top) and change in intense rain (RP10, all**

496 **three hydrological models, bottom)**

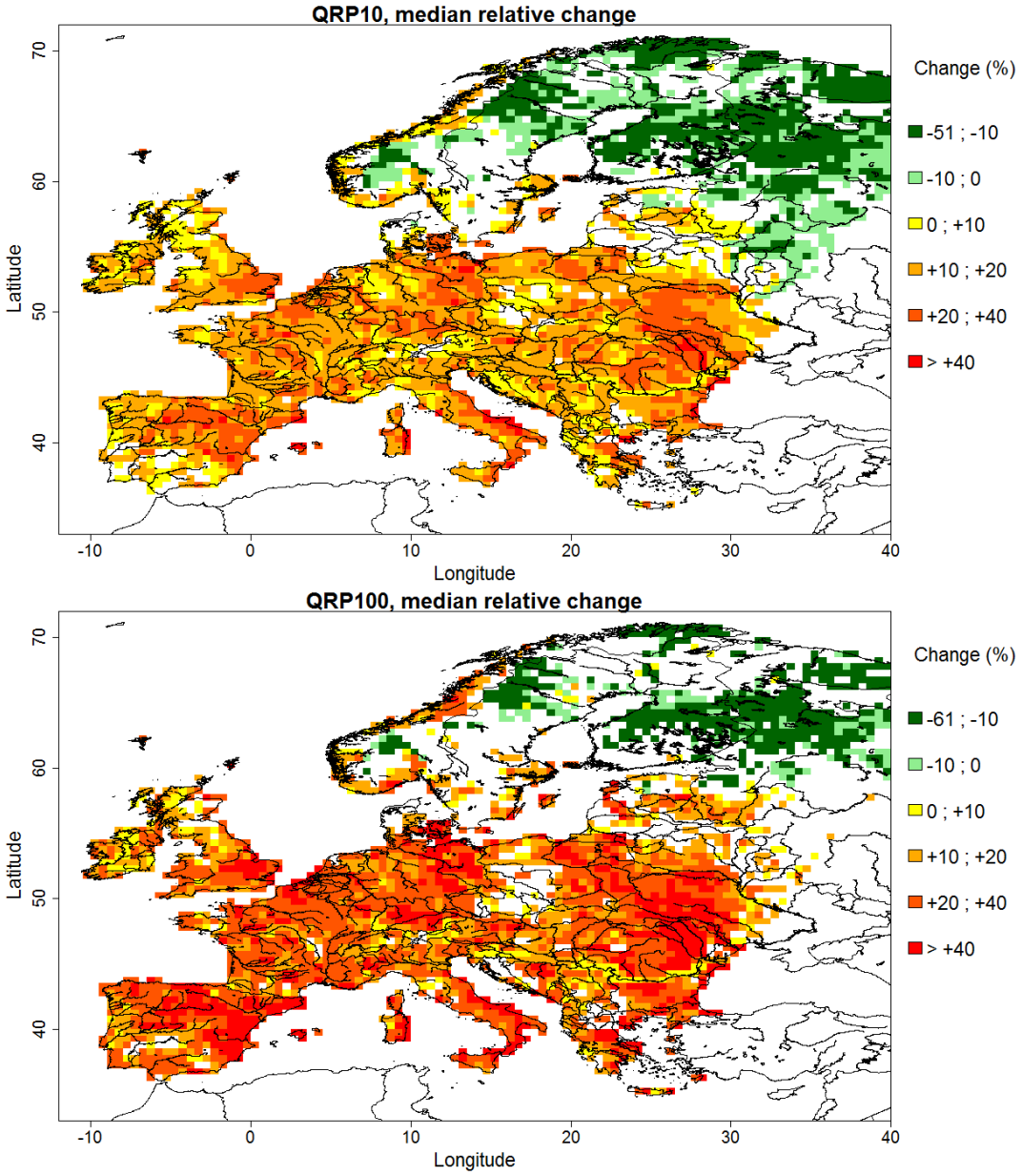

Figure 2: high flows median relative change, for two different return periods; RP10 (top), and RP100 (bottom). The median is computed over 33 members. Only significant changes (i.e. passing the Wilcox test at 5%) are shown here.

503

504

505

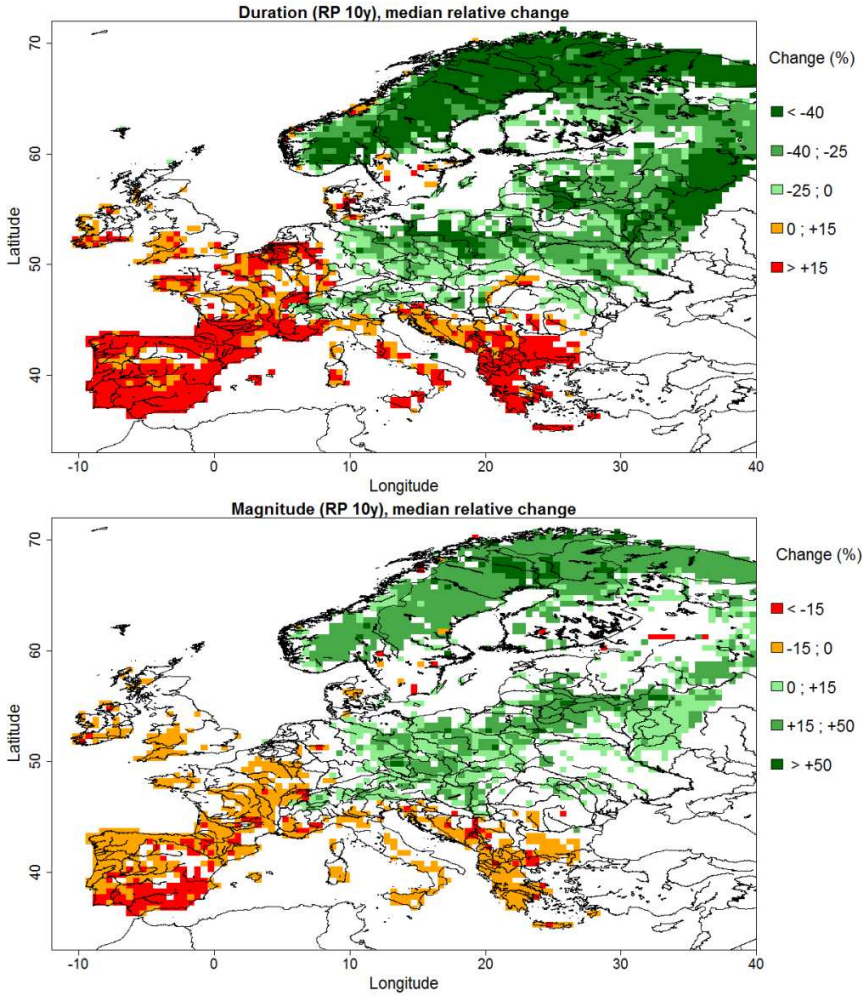

506

507 **Figure 3: characteristics of low flows (RP10): duration (top) and magnitude (bottom). The median is computed over 22**
508 **ensemble members. Only significant changes (i.e. passing the Wilcox test at 5%) are shown here. When QlowRP10 is zero for**
509 **the baseline period, we set the relative change as missing value.**

510

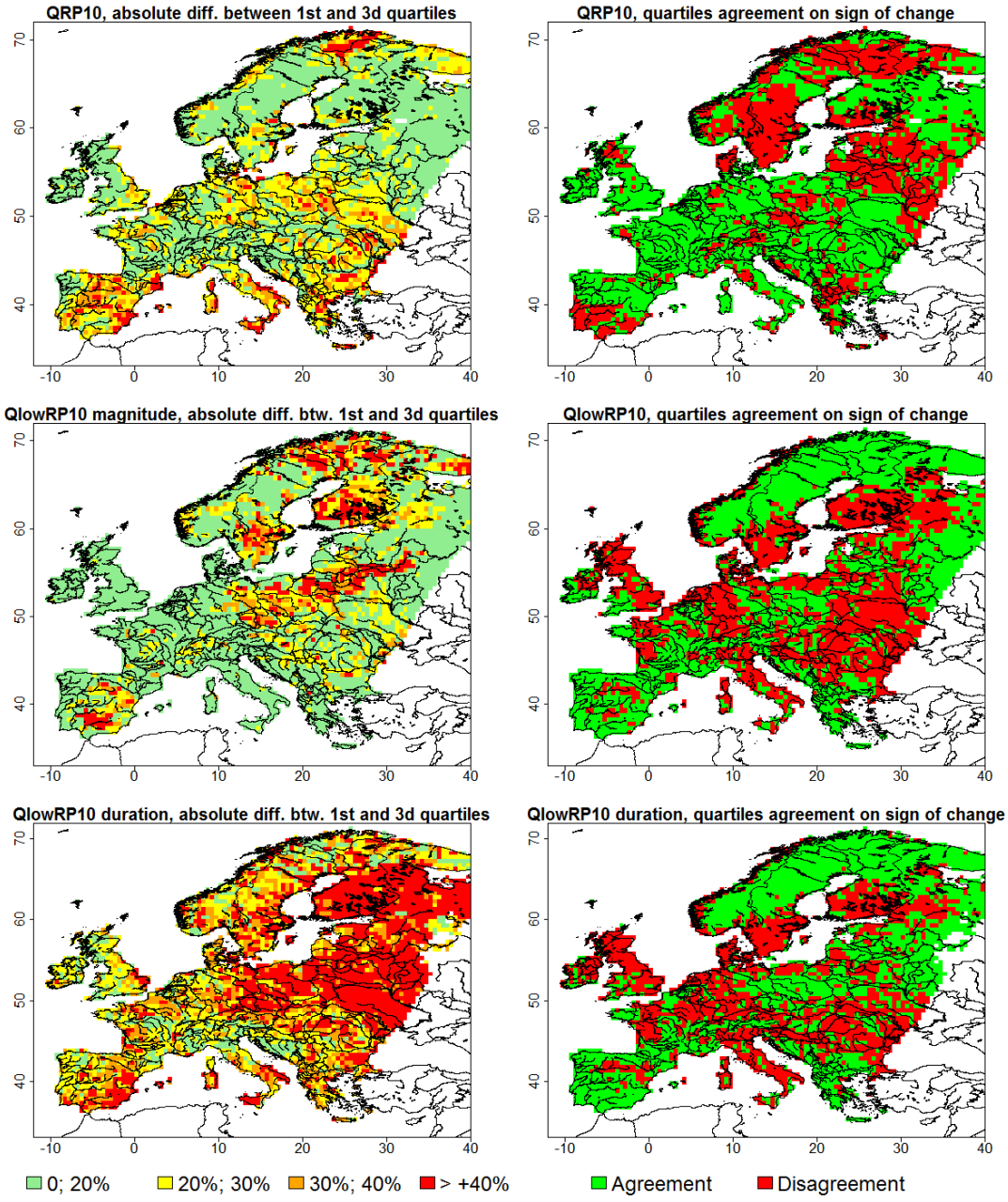

511

512 **Figure 4: quartiles of relative change. Left column: absolute difference between the 1st and 3rd quartiles of relative change (in**

513 **%) for QRP10 (top), QlowRP10 magnitude (middle) and QlowRP10 duration (bottom). Right column: agreement on the sign**

514 **of the 1st and 3rd quartiles (e.g. the green area means that both quartiles are positive or negative)**

515

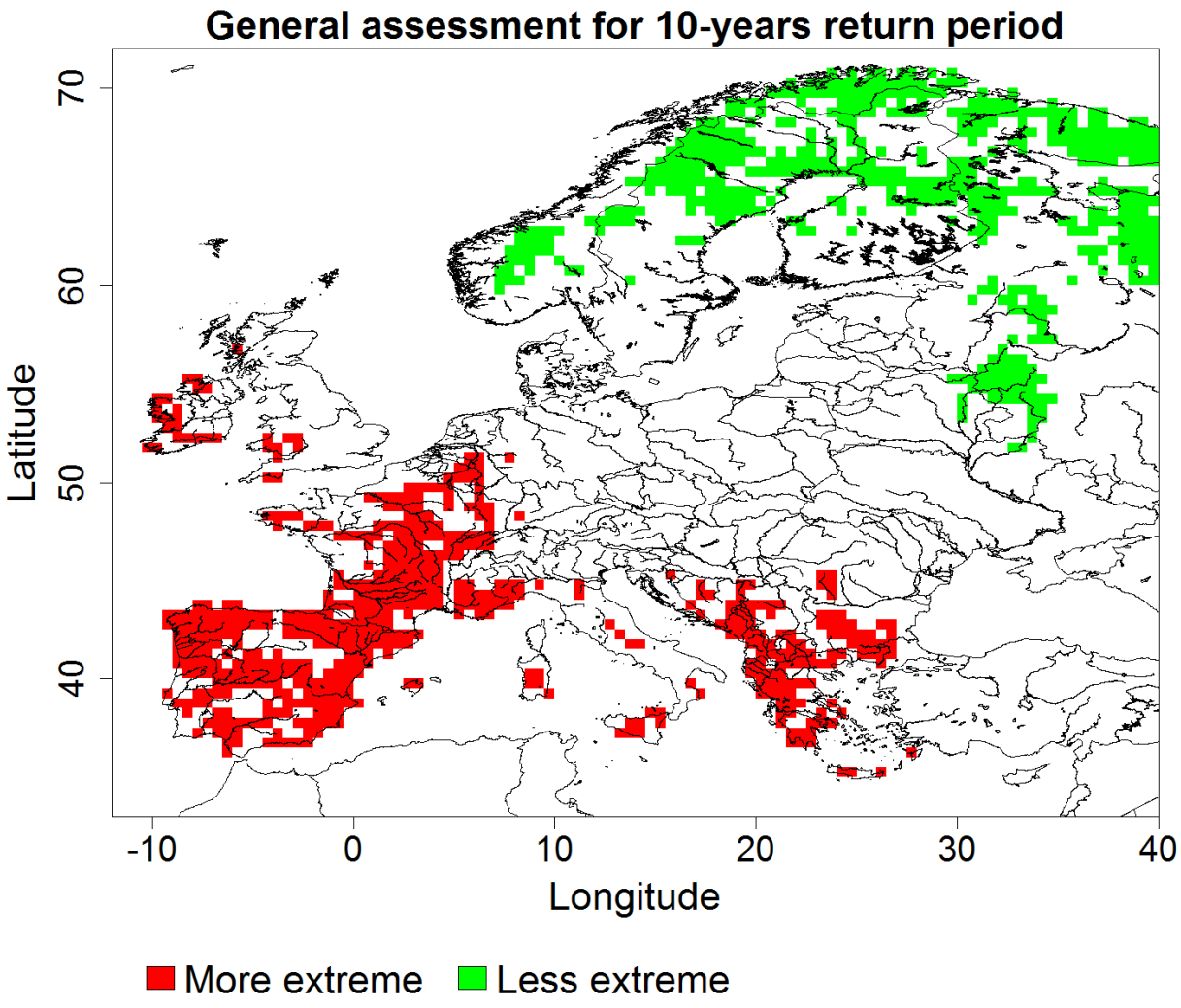

516

517 **Figure 5: summary of the impacts of extreme discharge (return period is 10 years) under a +2C warming. Green area means**
518 **that (i) QRP10 change < -5%, (ii) QRPlow10 change> +5% and (iii) QRPlow10 duration change <-5%. We show here only pixels**
519 **where all three change are statistically significant.**

520

521

522

523

Supplementary material

A1. Summary of models

- **E-HYPE**

The E-HYPE model (Donnelly et al., 2015) is a pan-European application of the Hydrological Predictions for the Environment (HYPE, Lindström et al. (2010)) which simulates hydrological variables in more than 35000 sub-basins (median size 200 km^2) across Europe. A modified Hargreaves-Semani equation using daily minimum and maximum temperature and a time constant radiation that is assumed to vary with latitude is used to compute evapotranspiration. Snow melt is calculated using a degree day method. In HYPE evapotranspiration, snow and runoff generation calculations are made for hydrological response units (HRUs) representing unique land use and soil type combinations and consisting of up to three soil layers down to 2.5 m. Each sub-basin may consist of any number of HRUs. The model is forced by daily precipitation and temperature and then calculates flow paths in the soil based on snow melt, evapotranspiration, surface runoff, infiltration, percolation, macropore flow, tile drainage, and lateral outflow to the stream from soil layers with water content above field capacity. HRUs are connected directly to the stream and act in parallel. The groundwater level in each HRU is fluctuating, may saturate the soil layers and water may percolate between sub-basins. Routing of the runoff is made along local and main rivers within each sub-basin and includes delay and dampening processes. Lakes, where they exist, cause delay of flow using the weir equation and may be local (off the main river) or main (on the main river).

- **LISFLOOD**

LISFLOOD is a GIS-based spatially-distributed hydrological rainfall-runoff model, which includes a one-dimensional hydrodynamic channel routing mode. Driven by meteorological forcing data (precipitation, temperature, potential evapotranspiration, and evaporation rates for open water and bare soil surfaces), LISFLOOD calculates a complete water balance at every daily time step and every grid cell defined in the modelled domain (current resolution is 5*5km). Basically, the model is made up of the following components: (i) a 2-layer soil water balance sub-model, (ii) sub-models for the simulation of groundwater and subsurface flow (using 2 parallel interconnected linear reservoirs), (iii) a sub-model for the routing of surface runoff to the nearest river channel, (iv) a sub-model for the routing of channel flow. The processes that are simulated by the model include snow melt, infiltration, interception of rainfall, leaf drainage, evaporation and water uptake by vegetation, surface runoff, preferential flow (bypass of soil layer), exchange of soil moisture between the two soil layers and drainage to the groundwater, sub-surface and groundwater flow, and flow through river channels. Runoff produced for every grid cell is routed through the river network using a kinematic wave approach.

- **VIC**

The Variable Infiltration Capacity model (VIC) performed calculations on a regular 0.5x0.5 degrees lat-lon grid. In VIC each grid cell is subdivided into an arbitrary number of tiles, each covered by a particular vegetation type. Evapotranspiration is computed for each tile, whereas the soil is uniform within each grid cell. The soil consists of 3 layers with a total depth of ~3 m for most cells. The energy balance approach of Penman-Monteith (Shuttleworth, 1993) is used to compute evapotranspiration, requiring a forcing consisting of atmospheric temperature and humidity, wind speed and incoming radiation. Penman-Monteith is also employed to simulate snow melt. VIC owes its name to the

568 treatment of surface runoff, which is generated from net precipitation under the assumption that the
569 infiltration capacity varies within each grid cell according to a one-parameter distribution function
570 (Wood et al., 1992). Routing of the runoff is taken into account with the model described in Lohmann et
571 al. (1996). This model first transports the runoff generated in a grid cell to the main river leaving the grid
572 cell with a unit hydrograph and then routs the water through the river network connecting the cells.

573

574

575

576

577

578

579

580

581

582

583

584

585

586 A2. Validation

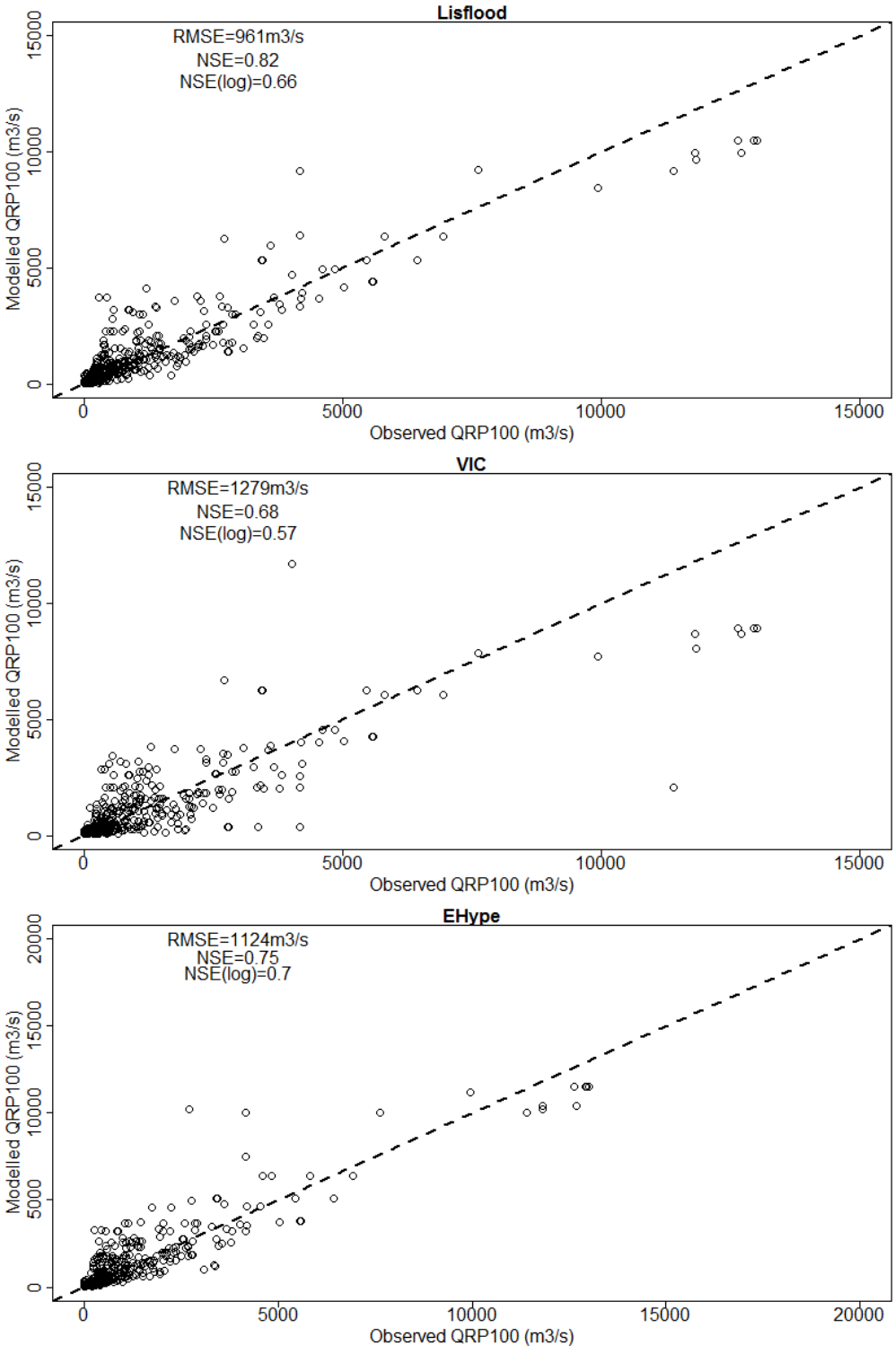
Lisflood
RMSE=961m3/s
NSE=0.82
NSE(log)=0.66
Modelled QRP100 (m3/s)
Observed QRP100 (m3/s)
VIC
RMSE=1279m3/s
NSE=0.68
NSE(log)=0.57
Modelled QRP100 (m3/s)
Observed QRP100 (m3/s)
EHype
RMSE=1124m3/s
NSE=0.75
NSE(log)=0.7
Modelled QRP100 (m3/s)
Observed QRP100 (m3/s)

587

588 **Figure S1: Observed QRP100 428 stations, years 1971/2000) vs. modelled one (median QRP100 over 5 climate members), for**
589 **each of the three hydrological models. The dashed line is y=x, NSE is Nash-Sutcliff Efficiency coefficient, NSE(log) is Nash-**
590 **Sutcliff Efficiency coefficient of log(observed QRP100) vs. log(modeled QRP100) and RMSE is the root mean squared error.**

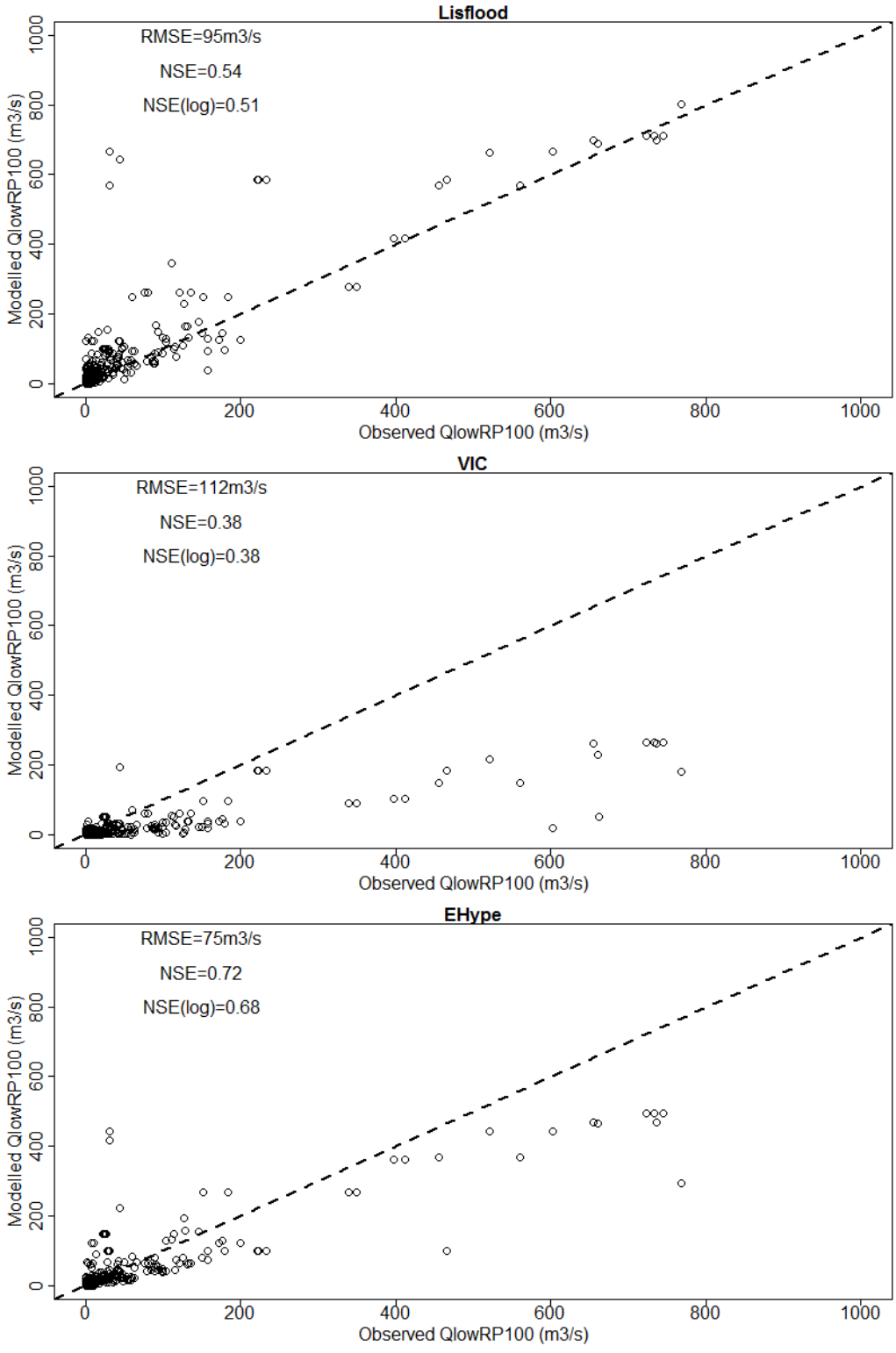

591

592 **Figure S2: same as Fig 1 but for QlowRP100**

A3. Floods, model by model, QRP10

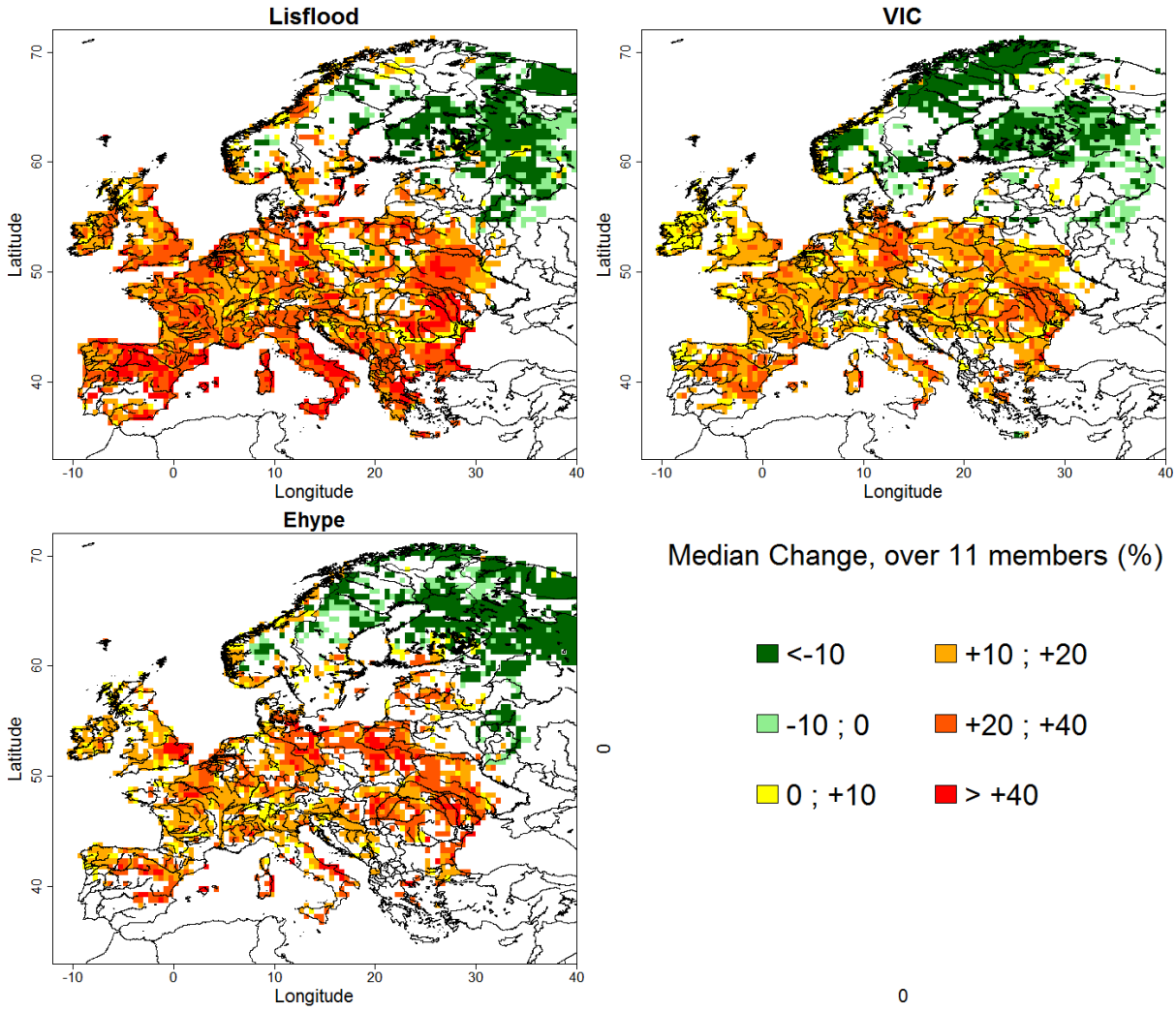

Figure S3: QRP10 median change for each of the 3 hydrological models. Median is computed over 11 members for each plot. Only significant changes are shown here.

601 A4. Evapotranspiration change, model by model

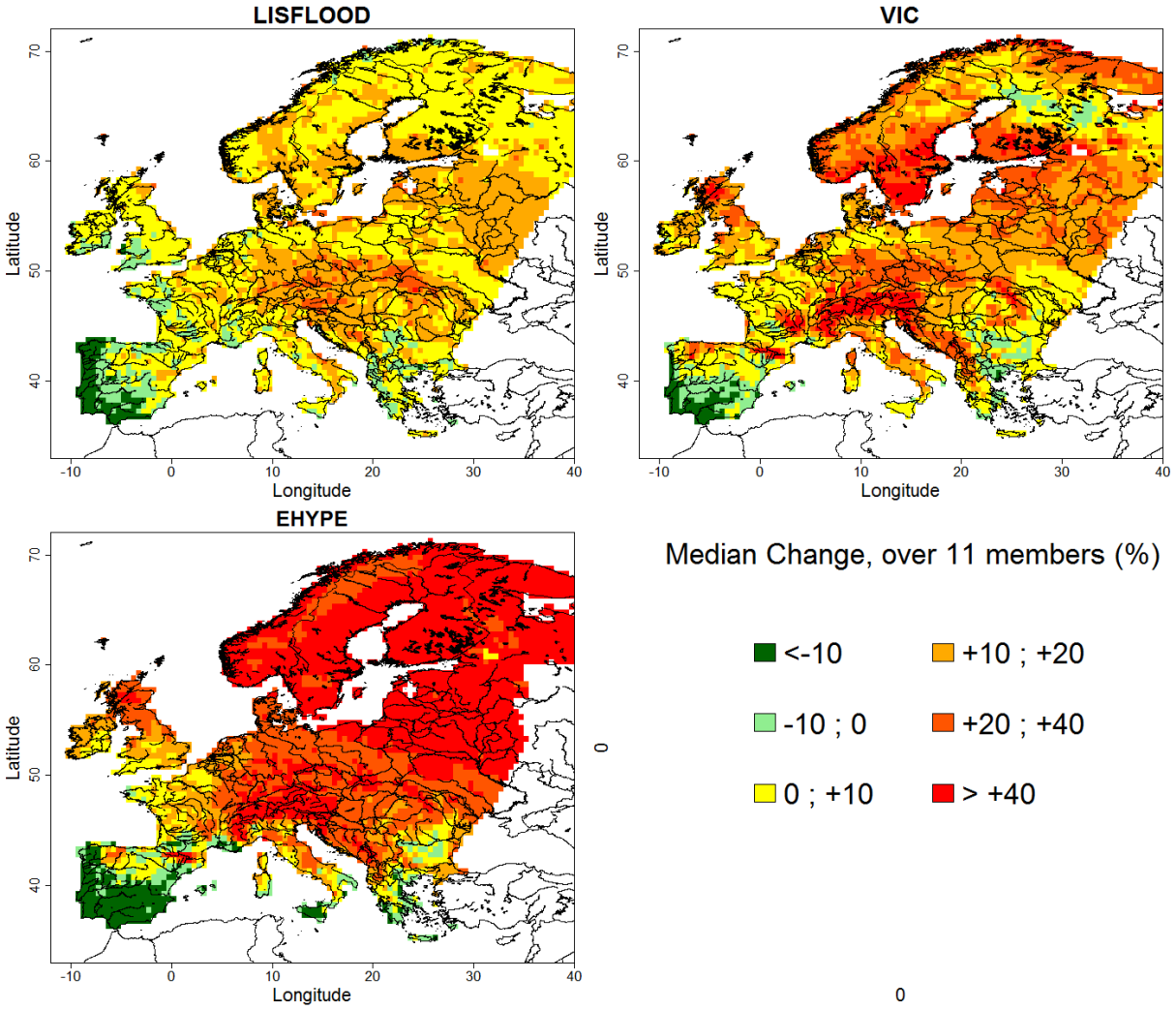

602

603 **Figure S 4: evapotranspiration relative change (%), for each of the three models. All pixels are shown.**

604

605 A5. Droughts magnitude, model by model

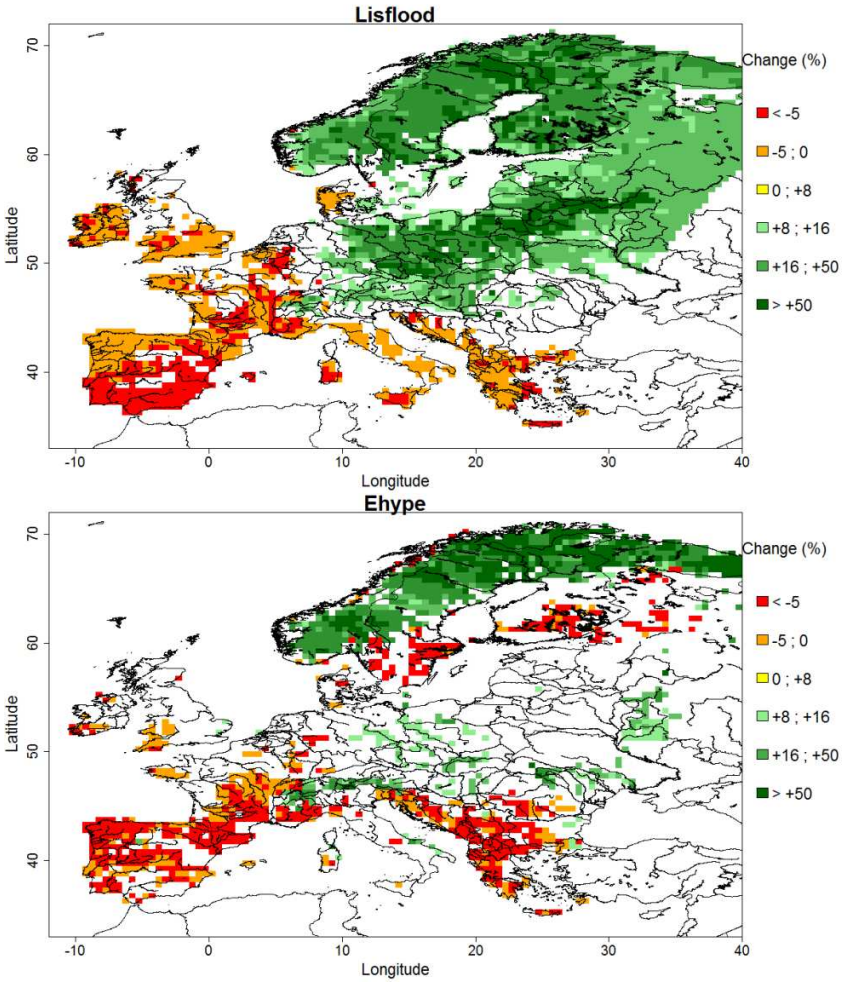

606

607 **Figure S5: QlowRP10 magnitude relative change, for both hydrological models used for low flows: Lisflood (top) and E-HYPE**
608 **(bottom). The median is computed over 11 members. Only significant changes are shown here. When QlowRP10 is zero for**
609 **the baseline period, we set the relative change as missing value**

610

611

612

613

614

615 A6. Drought magnitude and duration, RP100

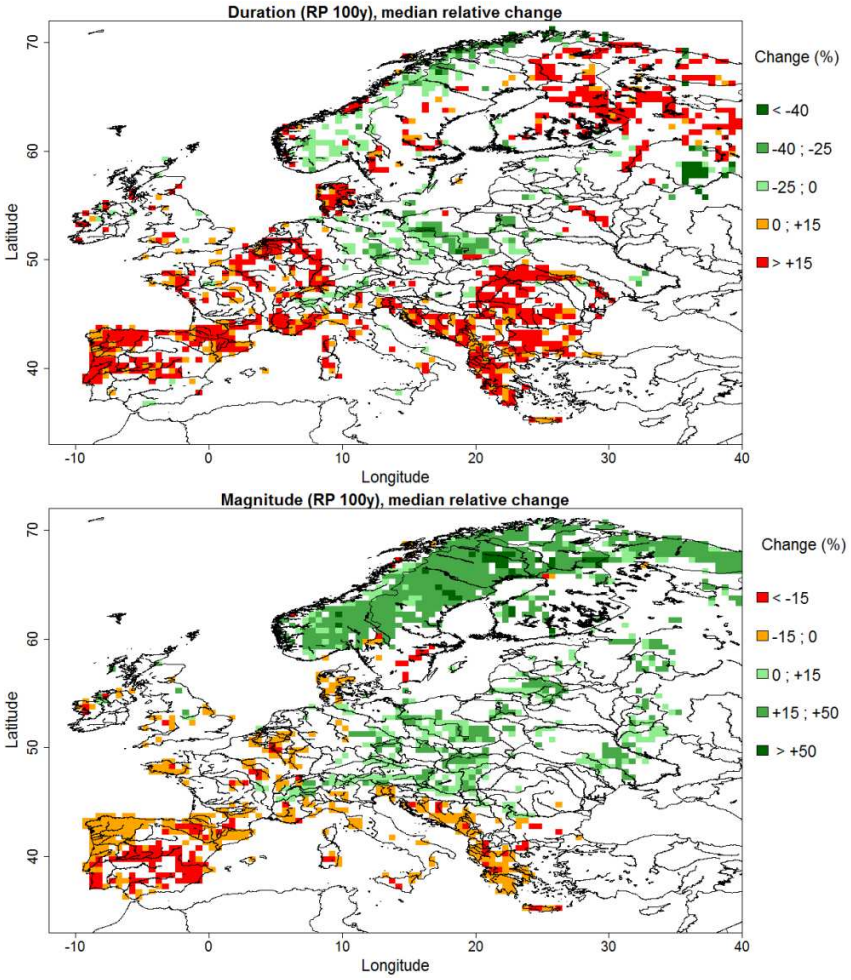

616

617 **Figure S 6: characteristics of low flows (RP100): duration (top) and magnitude (bottom). The median is computed over 22**
618 **ensemble members. Only significant changes are shown here. When QlowRP100 is zero for the baseline period, we set the**
619 **relative change as missing value.**

620

621

622

623

A7. 25th percentile and 75th percentile change

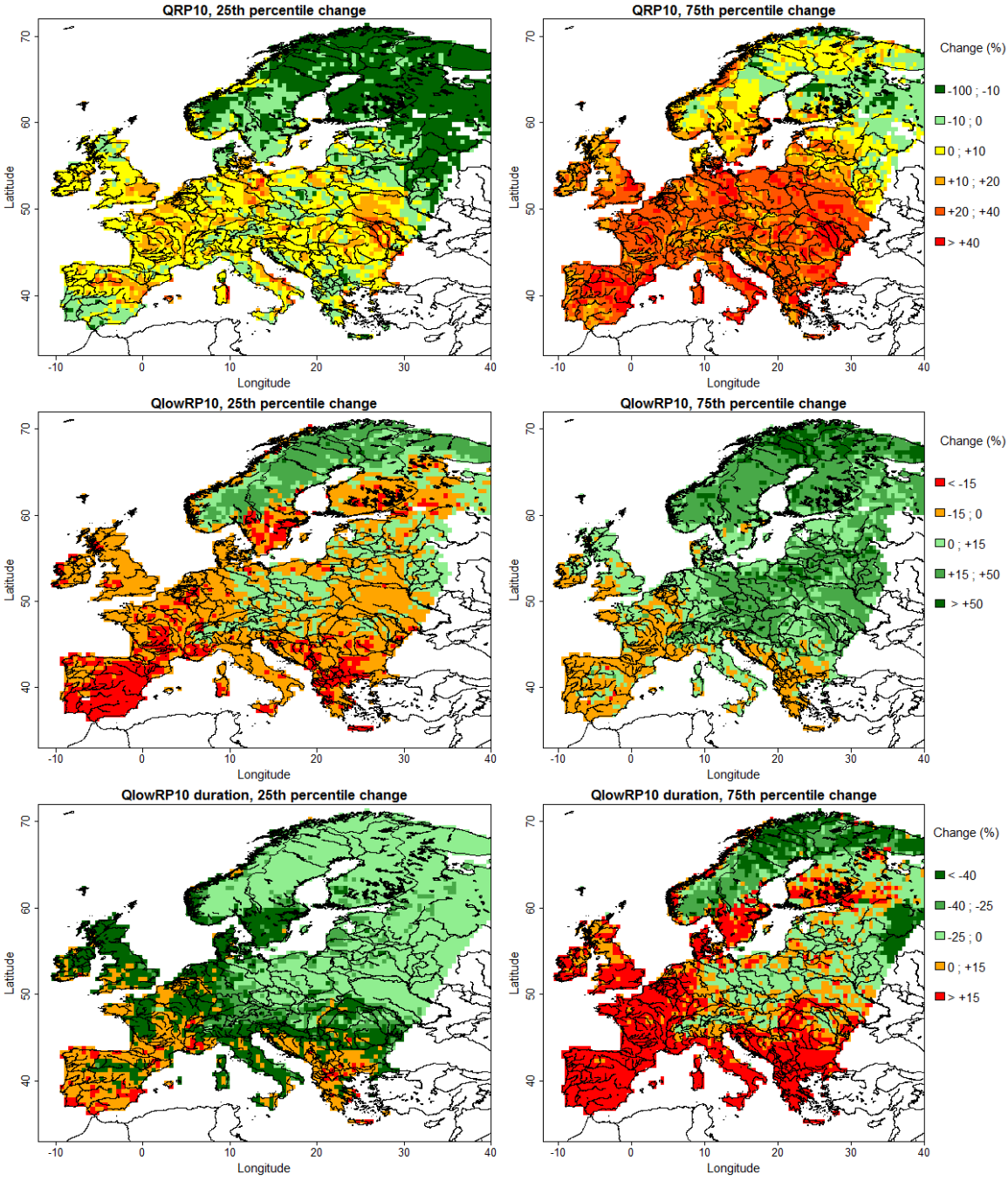

Figure S7: 25th percentile (left column) and 75th percentile (right one) relative change for QRP10 (top row), QlowRP10 (middle row) and QlowRP10 duration (bottom row). For each pixel, the percentiles are computed over 33 members (QRP10) or 22 members (QlowRP10 and QlowRP10 duration).

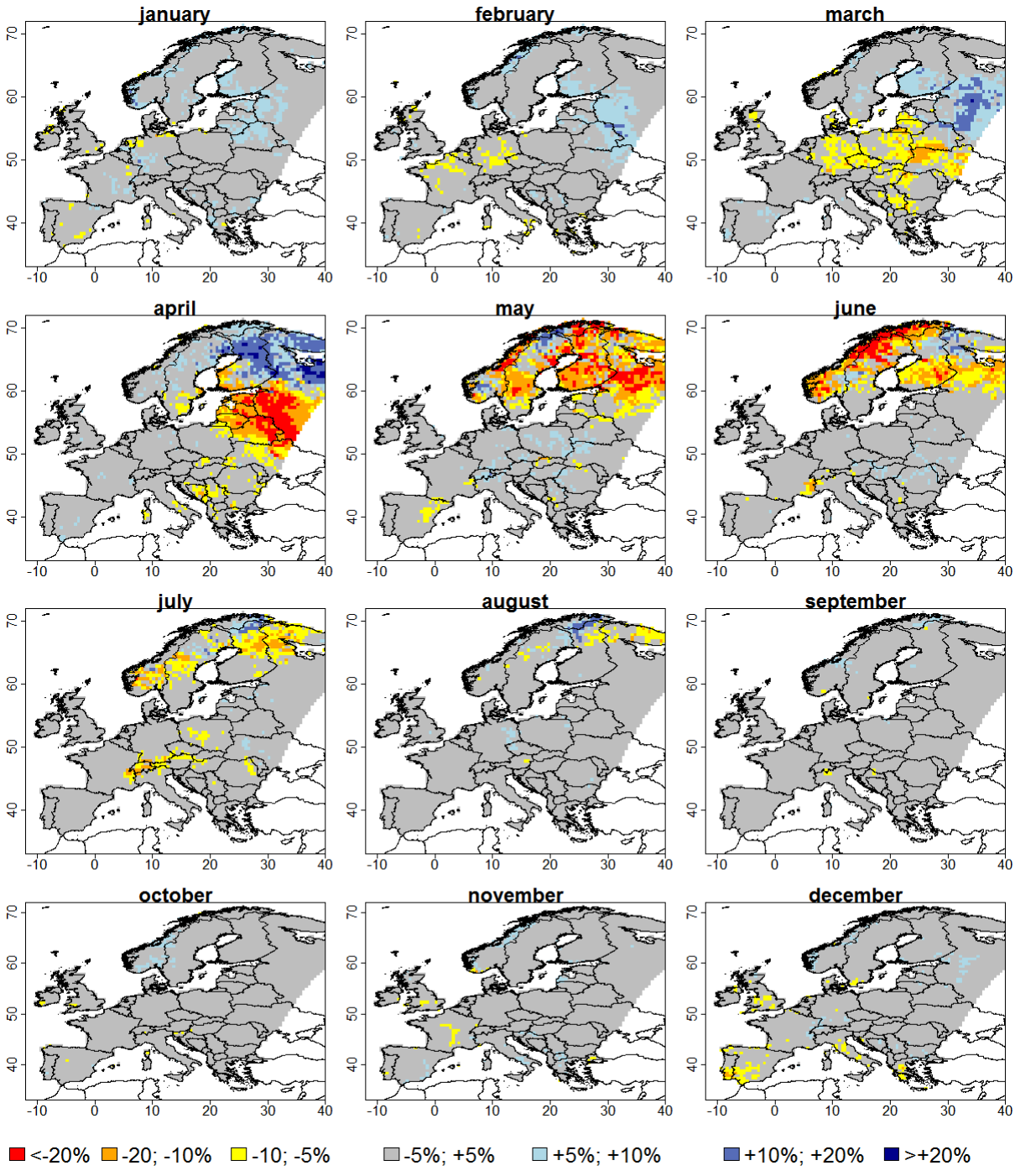

629

630 **Figure S8: relative change (%, between +2C period and baseline) in occurrence of maximum annual discharge, month by**

631 **month. Blue areas mean that in the future, according to the 33 members, the annual maximum discharge occurs more**

632 **frequently during the specific month.**

633 **References**

634 Donnelly C, Andersson JCM, Arheimer B (2015) Using flow signatures and catchment similarities to
635 evaluate the E-HYPE multi-basin model across Europe. Hydrological Sciences Journal:
636 doi:10.1080/02626667.2015.1027710
637 Lindström G, Pers C, Rosberg J, Strömqvist J, Arheimer B (2010) Development and testing of the HYPE
638 (Hydrological Predictions for the Environment) water quality model for different spatial scales.
639 Hydrology Research 41:295-319 doi:10.2166/nh.2010.007
640 Lohmann D, Nolte-Holube RALPH, Raschke E (1996) A large-scale horizontal routing model to be coupled
641 to land surface parametrization scheme. Tellus A 48:708-721
642 Shuttleworth WJ (1993) Evaporation. In: Maidment DR (ed) Handbook of Hydrology. McGraw Hill, New
643 York,
644 Wood EF, Lettenmaier DP, Zartarian VG (1992) A land-surface hydrology parameterization with subgrid
645 variability for general circulation models. Journal of Geophysical Research: Atmospheres (1984–
646 2012) 97:2717-2728
647

648

649